

Shortcut to Chemically Accurate Quantum Computing via Density-based Basis-set Correction

Diata Traore,^{1,2} Olivier Adjoua,¹ César Feniou,^{1,3} Ioanna-Maria Lygatsika,^{4,1,5}
Yvon Maday,^{4,6} Evgeny Posenitskiy,³ Kerstin Hammernik,⁷ Alberto Peruzzo,³
Julien Toulouse,^{1,6} Emmanuel Giner,¹ and Jean-Philip Piquemal^{1,3,*}

¹*Sorbonne Université, LCT, UMR 7616 CNRS, 75005 Paris, France*

²*Present address: Qubit Pharmaceuticals, Advanced Research Department, 75014 Paris, France*

³*Qubit Pharmaceuticals, Advanced Research Department, 75014 Paris, France*

⁴*Sorbonne Université, LJLL, UMR 7598 CNRS, 75005 Paris, France*

⁵*Present address: CEA, DAM, DIF, F-91297 Arpajon, France; and Université Paris-Saclay, LMCE, 91680 Bruyères-le-Châtel, France*

⁶*Institut Universitaire de France, 75005 Paris, France*

⁷*NVIDIA Corporation, Santa Clara, CA, USA*

Quantum computing promises a computational advantage over classical methods in electronic-structure calculations, with expected applications in drug design and materials science. Accessing a quantitative description of chemical systems while minimizing quantum resources, such as the number of qubits, is an essential challenge given the limited capabilities of current quantum processors. We provide a shortcut towards quantum computations at chemical accuracy by approaching the complete-basis-set limit (CBS) through integrating density-functional theory into quantum algorithms via density-based basis-set corrections coupled to basis-sets crafted on-the-fly and specifically adapted to a given system/user-defined qubit budget. The approach self-consistently accelerates the basis-set convergence, improving electronic densities, ground-state energies, and first-order properties such as dipole moments. It can also serve as a classical, *a posteriori*, energy correction to quantum hardware calculations. The strategy is assessed using GPU-accelerated state-vector emulation up to 32 qubits. We converge the ground-state energies of four systems (He, Be, H₂, LiH) within chemical accuracy of the CBS full-configuration-interaction reference, while offering a systematic increase of accuracy beyond a double-zeta quality for various molecules up to the H₈ hydrogen chain. We also obtain dissociation curves for H₂ and LiH that reach the CBS limit whereas for the challenging simulation of the N₂ triple-bond breaking, we achieve a near-triple-zeta quality at the cost of a minimal basis-set. This hybrid strategy allows us to obtain quantitative results that would otherwise require brute-force quantum simulations using far more than 100 logical qubits, thereby opening up opportunities to explore real-world chemistry with reasonable computational resources.

Quantum computing (QC) offers a promising approach to solving electronic-structure problems, with algorithms like Quantum Phase Estimation (QPE) and Variational Quantum Eigensolver (VQE) proving effective in performing ground-state quantum-chemistry wave-function calculations [1–6]. The electronic Hamiltonian is expressed in second quantization, employing an encoding that maps one spin-orbital to one qubit. This mapping allows one to represent an exponentially large Hilbert space using only a linear number of qubits. However, to achieve accurate and practically valuable predictions for chemical systems in real-world applications, the molecular Hamiltonian should be expressed and solved using extensive basis sets \mathcal{B} of orbital functions. The number of qubits required for such calculations quickly exceeds the available capacities on current Noisy Intermediate Scale Quantum (NISQ) devices, upcoming early Fault-Tolerant Quantum Computing (FTQC) devices, and high-performance classical emulators. Therefore, while chemistry has long been stated as a promising application for quantum computing, the endeavors have so

far been limited to small molecular systems and minimal basis sets. However, in practice, minimal basis sets fail to be predictive for ground-state energies and chemically useful calculations require at least significantly larger double-zeta basis sets. Requirements for computing molecular properties are even more drastic as they tend to converge more slowly with the size of the basis set than energies [7].

In electronic-structure theory, the exact solution is defined by the full-configuration interaction (FCI) method in the (infinite) complete-basis-set (CBS) limit. However, in practice, the solution derived from a finite basis set \mathcal{B} is used, which inherently suffers from truncation errors. This errors can be substantial for small basis sets, but for large enough basis sets it is possible to reach chemical accuracy, 1 kcal/mol (1.6 mHa), which is actually the target. Unfortunately, employing sufficiently large basis sets becomes very rapidly impractical for large systems, particularly those with more than a few dozen of light atoms. As a result, traditional quantum chemistry has developed a variety of methods to approach chemical accuracy at a reasonable cost.

In particular, basis-set correction techniques such as the density-based basis-set correction (DBBSC) method

* jean-philip.piquemal@sorbonne-universite.fr

[7–16], relying on density-functional theory (DFT), have proven effective not only for calculating ground- and excited-state energies, but also for determining dipole moments for a variety of systems including atoms, small organic molecules, and strongly correlated systems. To date, the DBBSC method has only been applied to still relatively large basis sets, and more specifically the family of Dunning basis sets [17], where chemical accuracy with respect to the CBS limit can be reached starting from a triple-zeta basis set. We note that the approximations developed within the DBBSC method target the CBS limit within a wave-function approach. This means that they do not address the intrinsic errors of the wave-function method itself, such as the effects of neglected excitation terms in truncated configuration-interaction (CI) or coupled-cluster methods.

Here, we propose the integration of the DBBSC method with quantum algorithms to expedite reaching the CBS limit and achieve chemical accuracy on large complex molecular systems. This strategy, which natively limits the required qubit counts, can be applied to quantum algorithms that tackle the ground-state quantum chemistry problem, such as the QPE or the VQE algorithms. While QPE can guarantee ground-state energy with arbitrary high precision given a carefully chosen initial state, it demands large quantum circuits and will only be viable in the FTQC era. Conversely, VQE lacks convergence guarantees but employs smaller circuits, aligning better with this study’s aim of advancing short-term quantum computers toward practical quantum chemistry applications.

In section I, we present two approaches (denoted “Strategy 1” and “Strategy 2”): 1) a basis-set correction *a posteriori* added to the solution of the quantum algorithm, integrating two contributions, namely the DBBSC correction developed in previous work [8] and a correction to the Hartree-Fock (HF) energy, and: 2) a self-consistent scheme [12] integrating the DBBSC method to the quantum algorithm that dynamically modifies the density-dependent terms in the Hamiltonian. Strategy 1 offers the possibility to correct any QC energy computation through an additive correction. Strategy 2 enables to self-consistently access an improved electronic density, offering improved energies and access to first-order properties.

These new methodologies enable the first investigation of DBBSC corrections in the minimal basis-set regime. To enhance further the accuracy of the DBBSC method beyond minimal basis sets, it is always possible to choose a larger basis set. In section II, we provide relevant tests using the main families of basis sets in Table II. Alternatively, in order to limit the qubit counts and to avoid the basis-set choice (which can be sometimes troublesome), we introduce a new strategy for defining compact adaptive basis sets. This on-the-fly approach is grounded on a pivoted Cholesky approach. We carried out numerical simulations using GPU-accelerated QC sparse emulation on up to 32 qubits, exploring the applicability of this

method to ground-state energies, dissociation curves, and dipole moments. We consistently observed significant improvements over typical quantum-algorithm approaches, reaching an accuracy level that would have otherwise required hundreds of qubits. We expect this to become part of a suite of ansatz improvements that will be employed in quantum-enhanced chemistry calculations while the two strategies based on the DBBSC method, particularly Strategy 1, can immediately provide improvements to existing results, with relatively simple effort.

I. METHODOLOGY

The overall procedure is illustrated in Figure 1. The procedure starts with the definition of the system and basis set such as STO-3G, 6-31G, or pcseg-0 [18]. Also, we introduce a new type of system-adapted basis sets (SABS) for Gaussian-type orbitals (GTOs), with size comparable to minimal basis sets, generated by taking as input the HF one-electron density of the system of interest at a fixed geometry (geometries and SABS used in this paper are available in the Supplementary Information (SI), see section VI A. and VI C.).

To build a SABS, the one-electron density is expanded on an accurate basis set, such as a Dunning basis set where the required number of qubits can reach the hundreds. This generation is based on the pivoted Cholesky decomposition (see mathematical details in Section ID), which is a theoretical tool commonly used to eliminate linear dependencies from a given basis set in *ab initio* electronic-structure theory [19–21]. In Table II and III, the SABS are labeled VXZ-Y where X is respectively D, T, Q, 5, or 6 for cc-pVDZ, cc-pVTZ, up to cc-pV6Z basis sets, and Y is the target size. In practice, the generated basis can have a larger size due to some additional constraints such as the need to keep the same basis functions for a given atom type particularly when spatial symmetries occur. We report in the SI the classically computed energies for the N₂, H₂O, LiH, and H₂ molecules.

We note that the adaptation and generation of basis sets to the molecular geometry has been the subject of several publications exploring other strategies. Among them, we can cite some recent works [22, 23], but also some other research in the context of quantum computing focusing on the need to limit the qubit requirements through basis-set reoptimization such as Refs. [24, 25]. Such reoptimizations cannot be performed on the fly and obtaining such improvements can take a large amount of time when dealing with large basis sets. Alternatively, Kottman and Aspuru [26] proposed a basis-set-free approach through an adaptive representation using pair-natural orbitals which was tested up to 22 qubits and potentially able to deal with systems in the range of 40 to 100 qubits.

After defining the second-quantized Hamiltonian, the quantum state is prepared on a quantum processing unit (QPU), using standard Hamiltonian mapping as Jordan-

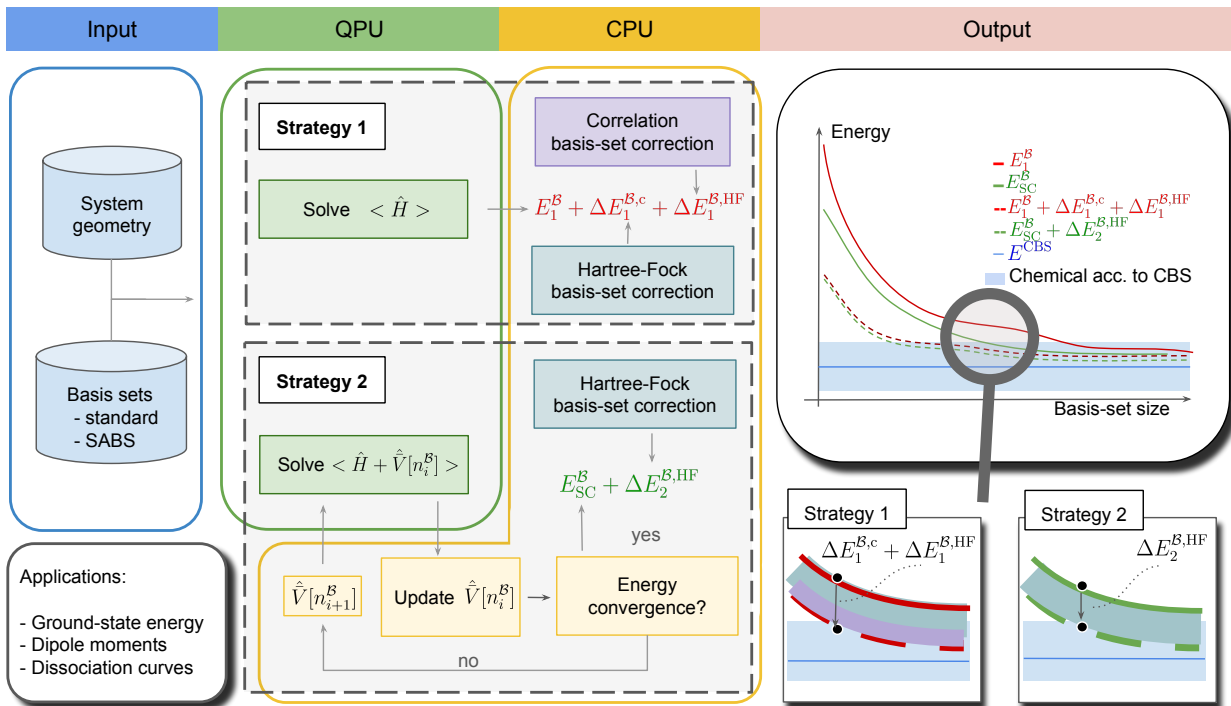


FIG. 1: **Architecture of the protocol introducing the DBBSC method to quantum computing.** Within this hybrid quantum-classical computing scheme, the QPU (Quantum Processing Unit) workload can be either performed by quantum hardware or replaced by a GPU-accelerated quantum emulator (GPU= Graphics Processing Unit, see section I.C.). The system and basis-set information are encoded in the quantum state. In Strategy 1, the QPU/GPU computes $\langle H \rangle$ and the non-self-consistent correlation correction and the HF basis-set correction are shifted to the CPUs (Central Processing Unit) of the classical compute node. In Strategy 2, the model includes a self-consistent basis-set correction potential which is iteratively optimized between QPU/GPU and CPU. The insets depict the effect of the corrections for the two strategies. One can choose either standard basis sets or SABS.

Wigner and Bravyi-Kitaev transformations (see SI, section II.). This step is followed by one of the two procedures labeled as “Strategy 1” and “Strategy 2”.

A. Strategy 1: *a posteriori* basis-set correction

“Strategy 1” relies on independent contributions of the quantum and classical computation parts, allowing applications to non-variational quantum algorithms. It can be used as an affordable and direct correction to any QC computation performed on real quantum hardware. The non-self-consistent correlation basis-set correction $\Delta E_1^{\mathcal{B},c}$ and the HF basis-set correction $\Delta E_1^{\mathcal{B},HF}$ are computed on classical computing units and added to the expectation value $E_1^{\mathcal{B}}$ coming out of the quantum solver. Therefore, the basis-set corrected energy in the basis set \mathcal{B} is approximated as

$$E_0^{\mathcal{B}} \simeq E_1^{\mathcal{B}} + \Delta E_1^{\mathcal{B},c} + \Delta E_1^{\mathcal{B},HF}. \quad (1)$$

We explicit the correction quantities in the following paragraphs and further details can be found in the SI

(see Section III).

1. Non-self-consistent correlation basis-set correction

The non-self-consistent correlation basis-set correction is a functional of the one-electron density $n^{\mathcal{B}}$,

$$\Delta E_1^{\mathcal{B},c} = \bar{E}^{\mathcal{B}}[n^{\mathcal{B}}], \quad (2)$$

and is built to correct the basis-set incompleteness due to short-range electron correlation in such a way that the correction correctly vanishes in the CBS limit: $\lim_{\mathcal{B} \rightarrow \text{CBS}} \bar{E}^{\mathcal{B}}[n^{\mathcal{B}}] = 0$. In this work, we use the approximation based on the Perdew-Burke-Ernzerhof (PBE) correlation functional introduced in Ref. [7]. We also discuss the choice of the approximation in the SI which we advise the reader to keep for a second reading as it does not add to the understanding of the procedure. However, we can mention here that the use of a better functional could give access to stronger-correlation regimes and further work on alternative approximations of the functional could allow applications on more complex systems. As

in the initial work of the DBBSC method [8], we use the HF density $n_{\text{HF}}^{\mathcal{B}}$ as an input density, leading to a correction with marginal computational cost with respect to the cost of calculating $E_1^{\mathcal{B}}$.

2. HF basis-set correction

The HF basis-set correction $\Delta E_1^{\mathcal{B},\text{HF}}$ corrects for the error in the HF energy occurring using a small basis set. Initial developments of the DBBSC approach were applied to relatively large basis sets where the HF energy has a maximum error of 0.1 mHa. For its application to quantum computations where minimal basis sets are usually chosen, the error within the HF energy is comparable to the electronic correlation error. However, this error is not taken into account in the DBBSC correlation approximations. A direct way to evaluate the HF basis-set correction $\Delta E_1^{\mathcal{B},\text{HF}}$ is to compute the difference between the HF energy in the CBS limit, that we estimate as the value E_{HF}^{5Z} obtained with cc-pV5Z basis set, and the HF energy $E_{\text{HF}}^{\mathcal{B}}$ in the basis set \mathcal{B}

$$\Delta E_1^{\mathcal{B},\text{HF}} = E_{\text{HF}}^{5Z} - E_{\text{HF}}^{\mathcal{B}}. \quad (3)$$

B. Strategy 2: Self-consistent basis-set correction

In ‘‘Strategy 2’’, we use the self-consistent version of the DBBSC method[8, 12]. In the approach, the Hamiltonian used in the quantum solver is

$$\hat{H} = \hat{H} + \hat{V}[n^{\mathcal{B}}], \quad (4)$$

where

$$\hat{H} = \hat{T} + \hat{V}_{\text{ne}} + \hat{W}_{\text{ee}}, \quad (5)$$

where \hat{T} , \hat{V}_{ne} , and \hat{W}_{ee} are respectively the kinetic, nuclei-electron interaction, and electron-electron interaction operators, and $\hat{V}[n^{\mathcal{B}}]$ is the one-electron basis-set correction potential operator,

$$\hat{V}[n^{\mathcal{B}}] = \int \bar{v}^{\mathcal{B}}[n^{\mathcal{B}}](\mathbf{r}) \hat{n}^{\mathcal{B}}(\mathbf{r}) d\mathbf{r}, \quad (6)$$

where $\bar{v}^{\mathcal{B}}(\mathbf{r})$ is the derivative of the correlation basis-set correction energy with respect to the density

$$\bar{v}^{\mathcal{B}}[n^{\mathcal{B}}](\mathbf{r}) = \frac{\delta \bar{E}^{\mathcal{B}}[n^{\mathcal{B}}]}{\delta n^{\mathcal{B}}(\mathbf{r})}, \quad (7)$$

and $\hat{n}^{\mathcal{B}}(\mathbf{r})$ is the density operator projected in the basis set \mathcal{B} . This potential, and therefore the Hamiltonian, is iteratively updated from the density $n_i^{\mathcal{B}}$ of the wavefunction ansatz solution of the i^{th} iteration. The communication of the updated Hamiltonian from the CPU to the QPU/GPU is done by using standard FCIDUMP files to communicate the one- and two-electron integrals to the

QPU/GPU software in order to construct the fermion operators. TREXIO files [27] are also useful to communicate a wider range of relevant information. The convergence criterion is reached when the difference between the last two iterations energies is less than 0.1 mHa. In practice, this is fulfilled after two iterations, and the self-consistent basis-set corrected energy $E_{\text{SC}}^{\mathcal{B}}$ is computed from the energy $E_2^{\mathcal{B}}$ coming out from the quantum solver as follows

$$E_{\text{SC}}^{\mathcal{B}} = E_2^{\mathcal{B}} + \bar{E}^{\mathcal{B}}[n^{\mathcal{B}}] - \int \bar{v}^{\mathcal{B}}[n^{\mathcal{B}}](\mathbf{r}) n^{\mathcal{B}}(\mathbf{r}) d\mathbf{r}. \quad (8)$$

The final energy including the HF basis-set correction is

$$E_0^{\mathcal{B}} = E_{\text{SC}}^{\mathcal{B}} + \Delta E_2^{\mathcal{B},\text{HF}}, \quad (9)$$

where the HF basis-set correction is identical to the one used in Strategy 1, i.e. $\Delta E_2^{\mathcal{B},\text{HF}} = \Delta E_1^{\mathcal{B},\text{HF}}$. Additional details can be found in the SI (see Section III).

C. Implementation: GPU-accelerated QPU emulation and shift of the DBBSC correction to classical resources

The DBBSC method does not increase the qubit count as the basis-set correction is performed classically using a density functional and a HF correction. In practice, such computations present no advantage to be performed at the QC level since they would consume a large number of qubits without accuracy benefit over its classical counterpart. Therefore a hybrid QC(ansatz)/DBBSC approach is highly preferable. Since it does not require much computational resources, ADAPT-VQE/DBBSC computations can be easily performed on a GPU-accelerated quantum emulator, the GPUs replacing the QPU. The DBBSC correction can be then shifted to the unused CPUs to maximize the computational efficiency while the computationally challenging ADAPT-VQE algorithm is fully offloaded on GPUs for optimal time-to-solution performances. Of course, the proposed extended hybrid ansatz schemes are also fully tractable on a real quantum computer, as the DBBSC correction can be entirely shifted to classical resources harnessing GPUs/CPUs to preserve the qubit count while the core ansatz is maintained on the QPU.

D. System-adapted basis-set generation

Within the DBBSC strategy, the natural choice for basis sets is the Dunning correlation-consistent basis-set family that offers a path to a fast CBS convergence, as demonstrated in initial DBBSC classical quantum-chemistry studies [7–16]. For quantum computing, such basis sets are unfortunately usually out of reach of quantum hardware/emulators as they are associated to very large qubit counts. In the present section and based on

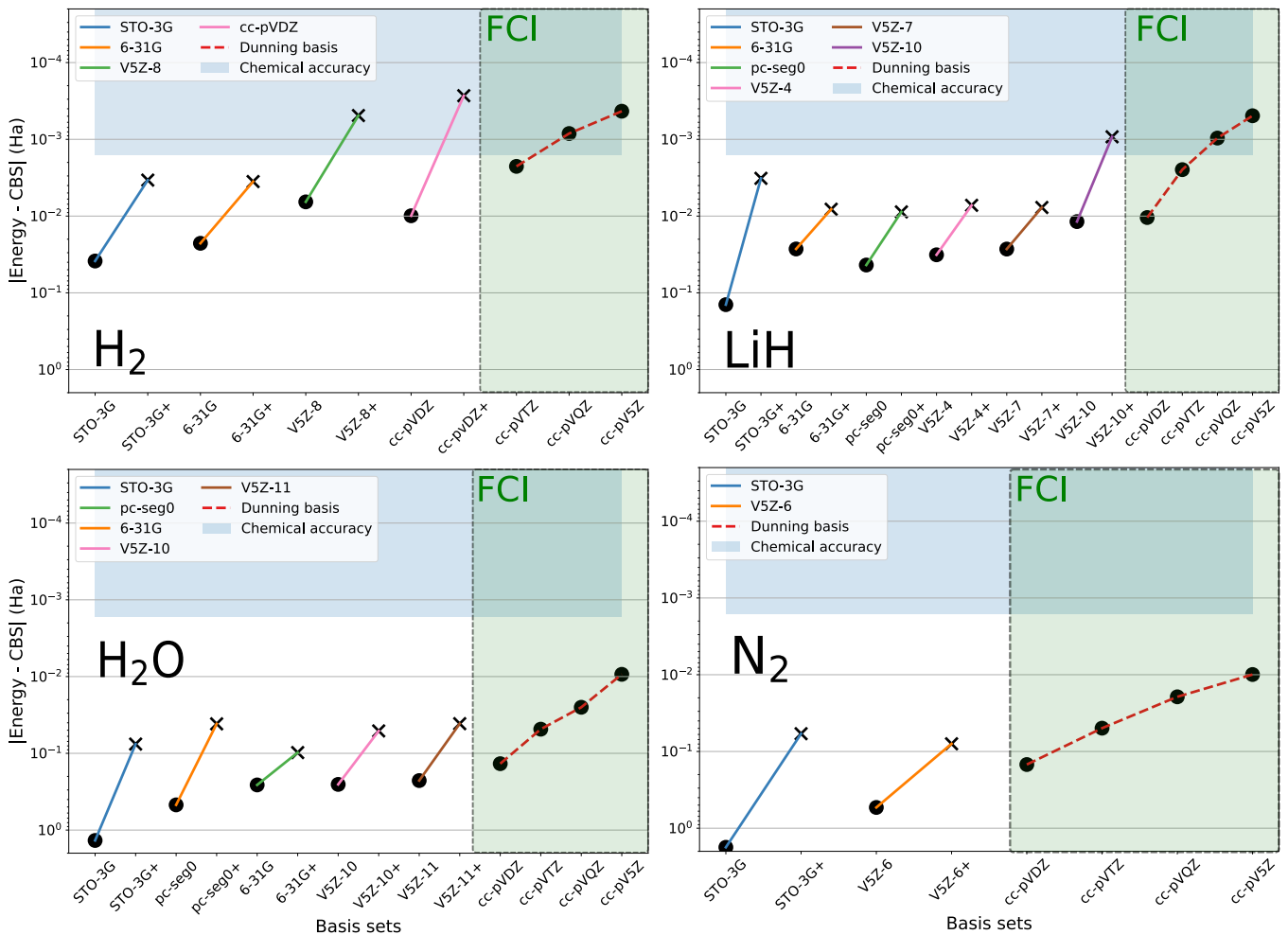


FIG. 2: Ground-state errors with respect to the extrapolated CBS limit. Outside the green box: ADAPT-VQE calculations. Inside the green box: FCI calculations from a classical computer. Dot markers correspond to energies without basis-set corrections. Cross markers correspond to energies corrected with Eq. 1. On the x-axis, the labels $\mathcal{B}+$ symbolize basis-set corrected values. The blue box corresponds to a range of 1.6 mHa around the extrapolated CBS limit. The errors for each ADAPT-VQE computations with respect to the FCI energy for a given basis set are reported in the SI.

these large Dunning basis sets, we address the task of generating atomic-orbital (AO) basis sets under a basis-size budget, with controllable accuracy [28]. We propose a mathematical formulation of this goal in terms of a constraint optimization problem, as follows.

Given a molecule composed of N_{atm} atoms, with fixed nuclear coordinates $\{\mathbf{r}_a\}_{1 \leq a \leq N_{\text{atm}}}$, let

$$\mathcal{B} := \{\chi_\mu\}_{1 \leq \mu \leq N_{\text{bas}}} = \bigcup_{a=1}^{N_{\text{atm}}} \{\chi_\mu^a(\mathbf{r} - \mathbf{r}_a)\}_{1 \leq \mu \leq N_{\text{bas}}^a}$$

denote a basis of atom-centered GTOs. It is assumed that an one-electron density, denoted by $n_0^{\mathcal{B}}$, is available after a converged ground-state energy minimization procedure (e.g. HF or CISD). Our main purpose is to *a posteriori* extract subsets of the given “large” basis set \mathcal{B} , denoted by $\mathcal{B}_I := \{\chi_\mu\}_{\mu \in I} \subseteq \mathcal{B}$ for any index sub-

set $I \subseteq \{1, \dots, N_{\text{bas}}\}$, achieving (i) a target size, and (ii) minimal accuracy loss on the given density $n_0^{\mathcal{B}}$, used as a reference. In the present computing scheme, since the DBBSC method uses the cc-pV5Z basis set for the HF basis-set correction, we choose $\mathcal{B} = \text{cc-pV5Z}$. In practice, this choice is motivated by the fact that such a quintuple-zeta basis fairly approaches chemical accuracy compared to quasi-exact all-electron numeric atom-centered orbital computations [29]. Hence, given a target basis size M smaller than N_{bas} , we seek the optimal index subset, denoted by I_M , that minimizes the *best approximation* error of the density $n_0^{\mathcal{B}}$ over the set of \mathcal{B}_I -representable one-electron densities, for any $I \subseteq \{1, \dots, N_{\text{bas}}\}$ with $|I| = M$, where $|\cdot|$ denotes the cardinal of a set, or, in other words, we solve an optimization problem under

constraints:

$$I_M := \arg \min_{I \subseteq \{1, \dots, N_{\text{bas}}\}} \min_{|I|=M} \|n_0^{\mathcal{B}} - n^{\mathcal{B}_I}\|, \quad (10)$$

where $\|\cdot\|$ is a given norm for functions over \mathbb{R}^3 . In the present work, we use the norm induced by the inner product $\langle u, v \rangle := \iint d\mathbf{r} d\mathbf{r}' \frac{u(\mathbf{r})v(\mathbf{r}')}{|\mathbf{r}-\mathbf{r}'|}$. Let us emphasize that (10) requires knowledge of the density $n_0^{\mathcal{B}}$, which is assumed to be pre-computed on a classical computer. Such quantity is available in the framework of the DBBSC scheme since HF computations are systematically performed at the cc-pV5Z level to estimate the CBS limit of the HF energy.

The problem in Eq. (10) can be solved as follows. Our approach is to identify a greedy procedure for discarding elements of the full AO-product set that spans the space containing the reference density $n_0^{\mathcal{B}}$, which admits the expansion

$$n_0^{\mathcal{B}} = \sum_{\mu, \nu=1}^{N_{\text{bas}}} D_{\mu\nu} \chi_{\mu} \chi_{\nu},$$

with $D = CC^{\top}$ the density matrix and C the orbital coefficients in the AO basis. We plan to achieve this by eliminating linear dependencies present in the AO-product set [21]. The pivoted Cholesky decomposition (PCD) of a matrix [30] is an algebraic tool for eliminating linear dependencies occurring between matrix rows (resp. columns), which may be interpreted as an iterative greedy procedure for discarding elements that do not contribute to the full row (resp. column) space, up to an orthogonal projection error tolerance. PCD has been previously applied to the auxiliary basis-set generation for density fitting [19–21]. In the present work, we employ PCD within a new scheme, named system-adapted basis-set (SABS) generation, for solving the problem in Eq. (10).

Let us formulate our scheme in detail. Prior to the AO-product selection and in order to ensure orbital symmetry of the resulting SABS, we pre-process the initial basis \mathcal{B} and first contract all angular components (e.g. all three p-type components p_x, p_y, p_z) of GTOs. To this end, we consider the partition $\{B_i\}_{i=1}^{N_{\text{orb}}}$ of $\{1, \dots, N_{\text{bas}}\}$, each B_i being an index block containing all angular components of a single GTO in \mathcal{B} , and the $N_{\text{orb}} \times N_{\text{bas}}$ contraction matrix P , defined for any $1 \leq i \leq N_{\text{orb}}$ as $P_{ij} = 1$ if $j \in B_i$ and zero otherwise. Next, we define the four-index tensor T with entries

$$T_{pqrs} := \sum_{\mu, \nu, \kappa, \lambda=1}^{N_{\text{bas}}} P_{p\mu} P_{q\nu} D_{\mu\nu} \langle \chi_{\mu} \chi_{\nu}, \chi_{\kappa} \chi_{\lambda} \rangle D_{\kappa\lambda} P_{r\kappa} P_{s\lambda},$$

and fold pairwise its first two and its last two dimensions, in order to form the $N_{\text{prod}} \times N_{\text{prod}}$ Gram matrix of weighted AO products, denoted by G , with $N_{\text{prod}} := (N_{\text{orb}})^2$. As a last pre-processing step, we discard rows

and columns of G corresponding to products made of components not centered on the same atom and denote the resulting submatrix A . Now, PCD is applied to A , using the machine epsilon as a tolerance threshold, yielding an index set sorted in pivot-descending order. Given a target M , we define the selected AO-product index set, denoted by S_M^{Chol} , as the M -first pivot indices. Lastly, we recover the underlying AO index set

$$J_M := \bigcup_{(p_1, p_2) \in S_M^{\text{Chol}}} \{p_1, p_2\}$$

and post-process it in order to ensure that the same GTO-parameter set is assigned to all atoms of the same chemical type. For this purpose, the new basis set associated to a chemical type is the union of parameters of those GTOs in \mathcal{B}_{J_M} that are centered on any atom of that type. This yields a solution $I_M \supseteq J_M$ to our problem in Eq. (10) and the resulting SABS is \mathcal{B}_{I_M} .

Note that our generation scheme directly fixes the size M of the selected products, i.e. $|S_M^{\text{Chol}}| = M$. The actual size of the AO basis set, equal to $|I_M|$, is only implicitly controlled during our procedure. In practice, as numerical results show, $|I_M|$ is very close to M for s- and p-type basis sets, while it remains the same order as M for higher orbital types. Overall, the GTOs SABS generation approach is extremely fast and offers access to compact basis sets, specifically adapted to a given system and user-defined qubit budget. Examples of SABS generation can be found in the SI (see Section VI.C.).

E. Computational Details

In the present study, to perform the ADAPT-VQE computations, we use the Qubit-Excitation-Based pool of operators, which is considered a standard [31]. Additional details about the ADAPT-VQE methodology can be found in the SI (see section II). ADAPT-VQE computations were performed using the Hyperion-1 GPU-accelerated state-vector sparse emulator [32] up to 32 qubits. Hyperion-1 uses classical computing systems and is grounded on an efficient multi-GPU (GPU=Graphics Processing Unit) ensemble of fast custom sparse linear algebra libraries accelerating Hyperion-1's exact/noiseless simulations. In this paper, computations were performed on NVIDIA DGX A100 nodes (8x 80GB A100 GPUs per node) and NVIDIA DGX H100 nodes (8x 80GB A100 GPUs per node). QC calculations being strongly memory-dependent, a single GPU can carry out 20 qubits ADAPT-VQE simulation depending on the nature (i.e. Hamiltonian sparsity) of the system whereas a single node (8 GPUs) can handle up to 28 qubits. Multi-node computations are required beyond such a qubit count. Further details about Hyperion-1 and its full capabilities will be given in a forthcoming publication. Convergence for ADAPT-VQE computation were set to 10^{-6} Hartree for all computations. Most computations started from

an HF initial state. For selected ones (indicated in the text and Tables), we started the ADAPT-VQE procedure from a non-converged perturbatively selected configuration interaction CIPSI [33] initial state (10^{-2} Hartree) to save some computational time within Hyperion-1. This reflects a commonly adopted strategy where a multi-determinant initial state is employed instead of a single HF determinant to increase the ground-state support of the initial state. The *Quantum State Preparation* of such classically-derived CIPSI wave-functions has been studied in the context of VQE [34] and QPE [35]. Also, we report in Table I, the walltime required for several ground-state energy calculations. As one can see, the walltime is not only a function of the number of qubits: sparsity is important. For example, the H_{12} Hamiltonian is sparser than the one of the water molecule resulting in faster convergence. Beside the increased computing power of H100 GPUs leading to improved time-to-solution, our results also highlight the importance of fast node-to-node interconnects when performing large scale quantum emulation. Indeed, the benefit of H100 over A100 is striking for the largest 32 qubits simulations on 16 nodes where a factor 3 improvement was observed on the DGX H100 systems. Such speedup is therefore also partially related to higher node-to-node bandwidth observed on DGX H100 versus A100 systems.

II. RESULTS

We computed the ground-state energies, dissociation curves, and dipole moments for the N_2 , H_2O , LiH, and H_2 molecules using both basis-set correction strategies. For all systems except H_2 , the 1s molecular orbitals were frozen, i.e. we use the frozen-core approximation. The error in each calculation is quantified as the deviation from the CBS limit, which itself is determined using a two-point extrapolation scheme, based on the cc-pVQZ and cc-pV5Z basis sets [36]. For the dipole-moment calculations we employed only Strategy 2, using an expectation value over the dipole-moment operator. The choice of this approach over a finite difference of energies is due to the lack of consistency guarantees, which arises from potential discrepancies in the treatment of the terms in the difference, thus leading to numerical errors [37]. The molecules selected for this study are commonly used in benchmarking quantum algorithms for chemistry due to their computational feasibility and the correlation strength they exhibit, which is representative of typical chemistry applications. Notably, these molecules have also been included in the systems used for benchmarking the DBBSC method in multiple studies [7–16].

The classical computations, including basis-set corrections and the calculation of reference energies and dipole moments, were carried out using Quantum Package 2.0 [38]. In this software, the FCI energies are approximated by the energy from a truncated configuration-interaction wave function, specifically CIPSI [39], to which a second-

order perturbation theory correction (PT2) is added. Given the demonstrated nearly-FCI quality of this approximation for the systems we studied, we simplify our terminology by referring to this approach as FCI rather than the more detailed CIPSI+PT2.

In this paper, we applied the basis-set corrections to the ADAPT-VQE algorithm implemented in our Hyperion-1 emulation software. Detailed technical specification are provided in the SI. Unless otherwise specified, the initial ansatz are HF wave functions. In instances where the ADAPT-VQE required an unreasonable amount of time to achieve convergence, we employed a cost-effective multi-determinant wave function as a starting point. In such cases, the number of determinants used are detailed in the notes of Table II.

A. Ground-state Energies

Ground-state energies are presented in Figure 2 and Table II. Details regarding the ADAPT-VQE iterations and the associated “ADAPT” values are provided in Fig. 1 to 14 in the SI, as long as additional tests on hydrogen chains and atoms. In Figure 2, a general trend is observed where the basis-set corrected energies align with value between the cc-pVDZ and cc-pVTZ levels, involving fewer than twenty qubits. As we can see from Table II, both strategies provide the same quantitative improvements. This shows that the results are consistent with the conclusion from Ref.[12] where the authors justified Strategy 1. We remind here that the basis-set correction does not fix the intrinsic error of the quantum algorithm.

We applied the basis-set correction strategies to systems with different correlation regimes, and for the best cases, we reach errors in the order of tens of mHa: 40 mHa for H_2O with 24 qubits, 60 mHa for N_2 with 16 qubits, and less than ten mHa errors for LiH and H_2 with less than 10 qubits. Without the basis-set correction, these results would have required more than a hundred of logical qubits. The results stay consistent for the other systems available in the SI (H_4 , H_6 , H_8). For H_2 using the cc-pVDZ basis set, the optimization reached chemical accuracy relative to the CBS limit, a process that used 20 logical qubits. Similar convergence to the CBS limit is observed for He and Be (see SI). Notably, this outcome contrasts with scenarios that typically require more than two hundred logical qubits. These results reflect findings from previous publications on the DBBSC method[8], where significant corrections typically begin with at least the cc-pVTZ basis set. Consequently, if one had access to a few hundred logical qubits, achieving chemical accuracy would be theoretically feasible for all presented cases. To support this claim, we have reported classically computed values for CIPSI energy corrections using Dunning basis sets (see Table 1 of the SI). According to this Table, the error relative to the CBS energy for the LiH molecule is 0.2 mHa with the cc-pVTZ basis set and both the correlation and HF basis-set corrections.

TABLE I: Walltime (in minutes) required to grow the wave-function ansatz of size N_{adapt} for a given molecular system using Hyperion-1 state-vector emulator on N_{gpus} NVIDIA GPUs. The results have been obtained on A100 (80 GB) and H100 (80 GB) GPUs using CUDA Toolkit 12.0 and NVIDIA HPC SDK 23.3.

Molecule	N_{adapt}	N_{qubits}	N_{gpus}	A100 walltime [min]	H100 walltime [min]
H ₂ O/6-31G	500	24	1	644	503
H ₁₂ /STO-3G	500	24	1	174	134
H ₁₄ /STO-3G	300	28	8	283	184
H ₁₆ /STO-3G	100	32	128	450	147

For H₂O, we achieve an error of 3 mHa from the cc-pVTZ basis set, and for N₂, the error is 1 mHa from the cc-pVTZ basis set. These results suggest that chemically relevant accuracies are achievable with around a hundred of logical qubits. However, the focus of our applications extends beyond simple energy calculations; we also examine energy derivatives through the dissociation curve, which will be discussed in the following part.

Since the discussed qubit counts were obtained using standard basis sets, we report in Table II computations using selected SABS basis sets for LiH, N₂, and H₂O. They were chosen to match the sizes of basis sets used in previous computations. Specifically for H₂O, employing the cc-pV5Z-10 basis (24 qubits) achieves results slightly superior to those obtained with the 6-31G basis set, using the same number of iterations. For H₂O, we observed a reduction in the HF correction by 40 mHa when moving from the 6-31G to the cc-pV5Z-10 basis, by over 100 mHa when comparing the STO-3G to the cc-pV5Z-4 basis for the LiH molecule, and more than an Hartree for the nitrogen molecule moving from the STO-3G to the cc-pV5Z-6 basis. Based on these findings, we anticipate that further exploration of this strategy could lead to a correction scheme requiring a single correction term. Of course, the interest of SABS is to be systematically improvable in the direction to the full accuracy of the corresponding Dunning basis set. It is important to note that this SABS systematic improvement is not limited to quantum algorithms such as ADAPT-VQE and is also present for the HF and FCI energies. Since the SABS approach strongly reduces the computational cost while maintaining accuracy, it should offer further applications of the CIPSI approach in classical quantum chemistry, especially when using the basis-set HF correction using large basis-set HF computations. In practice, a cc-pVTZ-like quality is reached (see Table II) for N₂ with a cc-pV5Z-11 basis set (32 qubits) and for H₂O with a cc-pV5Z-11 (30 qubits) basis set. A cc-pV5Z-10 basis set (28 qubits) achieves a cc-pV5Z-like ground-state energy accuracy for LiH. Overall, the SABS always provide the best SC-ADAPT solutions (i.e. before the HF correction). Finally, one last aspect of the analysis of such large basis-set simulations is related to the convergence of ADAPT-VQE. Indeed, in VQE-type computations [5], there is no formal guarantee of convergence and ADAPT-VQE belong to such heuristic family of methods. If, for

systems like H₂, LiH or N₂ (see SI, Figures 3-14), convergence is obtained in a few dozen of iterations, for more complex systems such as H₂O, the number of required iterations strongly increases when a double-zeta basis set is used. Clearly, Figure 2 in the SI shows that more than a thousand iterations would be required to achieve full convergence starting from the HF initial state. This heuristic aspect makes that no anticipation of the exact required number of iterations can be made. Moreover, if this could be fine on a real quantum processor, the use of classical emulation makes each iteration more costly in term of time-to-solution than the previous, limiting the overall convergence capabilities. It is possible to force convergence by replacing the HF starting point by a CIPSI one. Figure 2 in the SI shows that chemical accuracy can be easily reached with a well-converged CIPSI solution. However, ADAPT-VQE struggles to improve the solution which is expected due to the enormous size of the parameter space. Furthermore, the CIPSI-based initial state already contains significant amount of correlation. This represents a hard challenge for the ADAPT-VQE procedure, which now needs to more carefully pick the next ansatz operator to improve the existing quantum state. In any case, starting from an unconverged CIPSI wave function is a robust solution to strongly reduce the overall computational time. One example is given for H₂O and the V5Z-10 basis set which initially led to a not fully converged result. With a better CIPSI starting point, it is possible to recover a few milli-Hartrees (see numbers in parenthesis in Tab. II). It is also possible to change the operator pool but, the point here is that convergence becomes challenging when tackling complex electronic structures and such computations would not be possible without GPU-accelerated emulation. Overall, concerning the basis sets, it is important to point out a key anomaly, i.e. the remarkable performance of the minimal STO-3G basis set. This was expected as Pople already discussed the outperformance of this basis set in the seventies [40]. Indeed, Davidson and Feller detailed in their 1986 review [41] the existence of error compensations and stated that “the smaller the basis the more ab initio calculations assume an empirical flavor”. In practice, among the available minimal basis possibilities, STO-3G proved to be the most robust and cost-efficient choice for the DBBSC basis-set corrections. Also, in the DBBSC schemes, the STO-3G basis set highly benefits

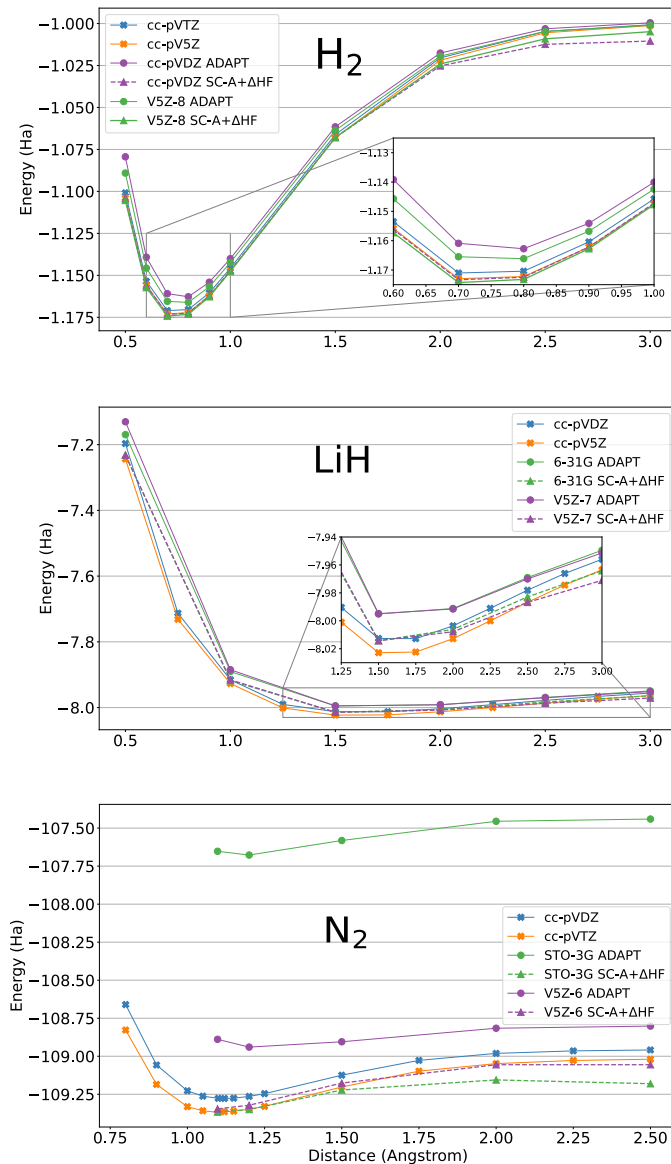


FIG. 3: Dissociation curves of H_2 , LiH and N_2 molecules. Blue and purple lines correspond to Dunning basis sets. Red and green plain lines correspond to ADAPT-VQE calculations without basis-set corrections. Red and green dash-dotted lines correspond to basis-set corrected dissociation curves.

from the HF basis-set correction which reduces as the basis set and number of qubits increases. When compared to SABS, for example, STO-3G always display smaller SC-ADAPT values and larger HF basis-set corrections. In practice, Pople also noted that STO-3G is especially good for energies around the minimum, and larger basis sets are clearly required to describe accurately the notoriously more difficult dissociation curves and dipole moments.

TABLE II: Ground-state energies (in Hartree) for H_2O , N_2 , LiH , H_2 , and H_8 calculated by FCI, ADAPT-VQE (denoted ADAPT), and basis-set corrected ADAPT-VQE according to Strategy 1 (denoted as $\text{A}+\Delta\text{c}+\Delta\text{HF}$) and to Strategy 2 (denoted as SC-A and SC-A+ ΔHF). Δc corresponds to the non-self-consistent correlation basis-set correction and ΔHF corresponds to the HF basis-set correction. The frozen-core approximation has been used for H_2O , N_2 , and LiH . The CBS limits are estimated by two-point extrapolations from cc-pVQZ and cc-pV5Z calculations. (1) Value between parentheses corresponds to a CI starting points with 11016 determinants selected with the CIPSI procedure.

H_2O	n_q	FCI	ADAPT	$\text{A}+\Delta\text{c}+\Delta\text{HF}$	SC-A	SC-A+ ΔHF
STO-3G	12	-75.01250	-75.01250	-76.30232	-75.197880	-76.30191
pcseg-0	24	-75.90855	-75.90843 ^a	-76.33681	-76.03999	-76.33279
6-31G	24	-76.11995	-76.11989 ^b	-76.28035	-76.23717	-76.32025
V5Z-10	24	-76.12626	-76.12409	-76.32705	-76.27418 (.27636) ⁽¹⁾	-76.32505
V5Z-11	30	-76.15902	-76.15165	-76.33704	-76.28622	-76.33570
VDZ	46	-76.24165	-	-	-	-
VTZ	114	-76.33250	-	-	-	-
VQZ	228	-76.35985	-	-	-	-
V5Z	400	-76.36877	-	-	-	-
CBS	-	-76.37812	-	-	-	-

N_2	n_q	FCI	ADAPT	$\text{A}+\Delta\text{c}+\Delta\text{HF}$	SC-A	SC-A+ ΔHF
STO-3G	16	-107.65251	-107.65251	-109.36630	-107.86974	-109.36661
V5Z-6	16	-108.88869	-108.88869	-109.34552	-109.09850	-109.34608
VDZ	52	-109.27698	-	-	-	-
VTZ	116	-109.37527	-	-	-	-
VQZ	216	-109.40558	-	-	-	-
V5Z	360	-109.41505	-	-	-	-
CBS	-	-109.42498	-	-	-	-

LiH	n_q	FCI	ADAPT	$\text{A}+\Delta\text{c}+\Delta\text{HF}$	SC-A	SC-A+ ΔHF
STO-3G	10	-7.88218	-7.88218	-8.02160	-7.89590	-8.02119
pcseg-0	14	-7.98139	-7.98139	-8.0160	-7.99166	-8.01561
6-31G	20	-7.99800	-7.99800	-8.01668	-8.00806	-8.01611
V5Z-4	10	-7.99287	-7.99287	-8.01758	-8.00562	-8.01690
V5Z-7	16	-7.99793	-7.99793	-8.01710	-8.01109	-8.01643
V5Z-10	28	-8.01302	-8.01302	-8.02575	-8.02134	-8.02540
VDZ	26	-8.01438	-	-	-	-
VTZ	86	-8.02234	-	-	-	-
VQZ	190	-8.02386	-	-	-	-
V5Z	290	-8.02433	-	-	-	-
CBS	-	-8.02482	-	-	-	-

H_2	n_q	FCI	ADAPT	$\text{A}+\Delta\text{c}+\Delta\text{HF}$	SC-A	SC-A+ ΔHF
STO-3G	4	-1.13415	-1.13415	-1.17606	-1.15590	-1.17594
6-31G	8	-1.15003	-1.15003	-1.16911	-1.16196	-1.16913
VDZ	20	-1.16275	-1.16275	-1.17239	-1.16858	-1.17246
V5Z-8	24	-1.16613	-1.16613	-1.17315	-1.17170	-1.17320
VTZ	56	-1.17041	-	-	-	-
VQZ	120	-1.17182	-	-	-	-
V5Z	220	-1.17223	-	-	-	-
CBS	-	-1.17265	-	-	-	-

H_8	n_q	FCI	ADAPT	$\text{A}+\Delta\text{c}+\Delta\text{HF}$	SC-A	SC-A+ ΔHF
STO-3G	16	-4.24339	-4.24320	-4.45483	-4.32764	-4.45354
6-31G	32	-4.37032	-4.35752	-4.43488	-4.41275	-4.43502
VDZ	80	-4.42756	-	-	-	-
VTZ	222	-4.47121	-	-	-	-
VQZ	474	-4.47702	-	-	-	-
V5Z	864	-	-	-	-	-
CBS	-	-	-	-	-	-

^a 500 iter. with 14668 CI selected with the CIPSI procedure for the initial state.

^b 1000 iter. with 10879 CI for the initial state.

TABLE III: Dipole moments of H₂O and LiH, frozen core calculations, FCI, and self-consistently basis-set corrected ADAPT-VQE (noted SC-A) in atomic units. Δ HF corresponds to the HF basis-set correction to the dipole moment. We use the difference between the aug-cc-pV5Z Hartree-Fock dipole moment with the Hartree-Fock dipole moment in the basis of interest to compute Δ HF. Details are available in Table 5 of the SI.

LiH	n _q	FCI	SC-A	SC-A+ Δ HF
sto-3G	10	-1.81835	-1.86299	-2.31321
pcseg-0	14	-2.33313	-2.37289	-2.25650
6-31G	20	-2.16646	-2.20768	-2.23674
V5Z-4	10	-2.37818	-2.44145	-2.22886
V5Z-7	16	-2.23095	-2.27789	-2.25618
V5Z-10	28	-2.24997	-2.27458	-2.31438
cc-pVDZ	26	-2.25566	-	-
cc-pVTZ	86	-2.29998	-	-
cc-pVQZ	190	-2.30361	-	-
cc-pV5Z	290	-2.30647	-	-

H ₂ O	n _q	FCI	SC-A	SC-A+ Δ HF
sto-3G	12	-0.63584	-0.67084	-0.77162
pcseg-0	24	-0.95822	-0.99450	-0.77065
6-31G	24	-0.99020	-1.01898	-0.76342
V5Z-10	24	-0.99305	-1.01887	-0.77634
V5Z-11	30	-0.99185	-1.02170	-0.77737
cc-pVDZ	46	-0.76073	-	-
cc-pVTZ	114	-0.75013	-	-
cc-pVQZ	228	-0.74994	-	-
cc-pV5Z	400	-0.74241	-	-

B. Dissociation Curves

We pursue with the dissociation energies reported in Figure 3. Clearly, the simple ADAPT-VQE/STO-3G level of theory (see Figure 3 and Table II) appears quite far from an accurate description of the systems dissociation (i.e. compared to the largest basis sets), which starts with FCI/triple-zeta (and beyond) levels. The non-corrected ADAPT-VQE values are represented with bold lines whereas the corrected values are reported with dashed curves. These dissociation curves are extremely challenging as they require to capture both electronic correlation and HF basis-set corrections. First, we notice that for all the cases, the corrected values around the equilibrium are always substantially closer to the large cc-pV5Z reference basis-set values than the uncorrected ones and improve with the basis-set size and the use of SABS. For longer-range distances, the basis-set requirements appear even more stringent. In practice, the 3 dissociation curves manage to converge to high accuracy thanks to the use of SABS: nearly a triple-zeta quality for N₂ (using a corrected cc-pV5Z-10 basis), nearly to a cc-pV5Z quality for H₂ (using a corrected cc-pV5Z-8 basis) and nearly a cc-pV5Z for LiH (using a corrected cc-pV5Z-8 basis). For H₂, the corrected cc-pVDZ curve matches the cc-pV5Z reference until 2.5 Angstrom and a slight discrepancy appears at long range. This is consistent with classical computations leading to a CBS con-

vergence with a corrected cc-pVTZ basis (114 qubits). It is possible to fix this issue more affordably by enriching ADAPT-VQE using a cc-pV5Z-8 basis requiring only 24 qubits. For LiH, it is also possible to fix the small discrepancies observed on the cc-V5Z-7 basis-set dissociation curve using a larger cc-V5Z-10 (28 qubits) basis which converges to the CBS limit. Finally, it is important to highlight the good DBBSC performance for the prediction of the triple-bonded N₂ dissociation curve. Indeed, such computation is well-documented in the literature and known as extremely difficult as it requires both a multi-reference treatment and core-valence basis sets [42–44]. At the cost of a minimal basis set (i.e. 16 qubits), our N₂ DBBSC computations achieved nearly a triple-zeta (cc-pVTZ) quality providing an accuracy which would have required around 100 logical qubits in the context of a brute-force simulation. To the best of our knowledge, these results are the most accurate using a quantum algorithm when compared to the most recent results from the literature. Indeed, a group of researchers managed to predict such dissociation using a Local Unitary Cluster Jastrow (LUCJ) ansatz coupled to double-zeta basis sets (6-31G and cc-pVDZ) [45]. The computation required the use of massive computational resources, namely hundreds of compute nodes of the Fugaku classical supercomputer coupled to a QPU. Alternatively, in the context of the fermionic quantum emulator, N₂ simulations used ADAPT-VQE coupled to the 6-31G and def2-SVP (56 qubits) basis sets to perform computation via approximate Matrix Product States (MPS) [46]. We achieved a better accuracy with far less qubits and, again, these results can be systematically improved using larger SABS. Indeed, going beyond a cc-pVTZ basis set is possible using the next (larger) SABS in term of size: cc-pV5Z-11 (32 qubits).

C. Dipole Moments

We also explored the idea to extend the basis-set correction schemes to molecular properties such as the dipole moment. We report in Table III the dipole moments of H₂O and LiH. In practice, it is known that dipole moments require the addition of diffuse functions for which the DBBSC approximation does not correct. However, according to Ref. [47], the rate of convergence of the dipole moment with the basis size should be the same as for the energy. Therefore, it is relevant to apply the basis-set correction to the dipole moment. Here, the chemical accuracy refers to the best estimation provided using the cc-pV5Z basis set. They are computed in the classical software from the density out of the last ADAPT-VQE run. From Table III, the second strategy leads to dipole moments with errors slightly superior to FCI dipole moments. However, the addition of the HF basis-set correction permits to reach dipole moments comparable to the double-zeta calculations for both systems. It is important to note that the observed ADAPT-VQE slow con-

vergence in term of iterations is the source of the small errors. For LiH, the STO-3G dipole moment reaches an error of 0.01 atomic units. For H₂O, the error is reduced to 0.01 atomic units with respect to the cc-pVDZ value which has an error of 0.2 atomic units. In all cases, strong improvements are observed with respect to the STO-3G/ADAPT-VQE level. Further improvements are observed as the size of the basis sets increases.

III. CONCLUSION

We demonstrated the applicability of the DBBSC method to quantum computing algorithms for chemistry. Using ADAPT-VQE, these approaches were shown to be able to systematically improve STO-3G minimal basis-set results by predicting total energies that are intermediate between double-zeta and triple-zeta FCI qualities. Overall, the presented self-consistent total energies are fully in line with their *a posteriori* counterparts, opening therefore a path towards computations of properties thanks to the availability of improved QC densities. As the *a posteriori* approach can be virtually applied to any QC computation performed on real hardware via classical computing, it provides an affordable improvement strategy of current QC computations. Triple-zeta accuracy can be achieved using double-zeta basis sets or by using our SABS approach. Such “black-box” pivoted Cholesky strategy for the on-the fly generation of basis sets has been shown to be competitive and often superior to available standard choices while offering systematic computational savings over large basis sets reducing therefore significantly the qubit requirements. Their usefulness is therefore not limited to quantum computing algorithms as they also offer systematically improvable solutions for performing reference classical computations. Indeed, since SABS are user-defined truncated versions of the Dunning basis sets that can match a qubit budget, they offer a reduced cost access to improved accuracy for any quantum chemistry method. Overall, the DBBSC method allows for a partition of the Hilbert space treatment which can remain handled by the QC ansatz embedded in an effective DFT correction dealing with the missing short-range electron correlation effects while the missing HF basis-set correction energy is obtained via a computationally affordable process. In such a framework, the two parts of the basis-set correction do not require to be evaluated at the QC level and can be fully shifted to classical computing while retaining the core QC algorithm features at a constant qubit count. The strategy allows us to access an improved electronic density thanks to a self-consistent scheme opening a path for the evaluation of first-order properties such as dipole moments. Of course, since the approach is hybridized with DFT, it is focused on improving the density and does not provide the exact many-body wave function. However, it provides an accelerated basis-set convergence, strongly improves the solutions and allows us to compute chemi-

cally meaningful energies and properties on systems that would have required far more than 100 logical qubits. We also verified that the correction gets smaller and smaller as the basis set increases so it has the correct CBS limit. Consequently, using a DBBSC/SABS approach, the computation of the H₂ total energy at the FCI/CBS level that would have required more than 220 logical qubits, i.e. the qubit count needed to perform at least a FCI/cc-pV5Z computation, can be achieved here with only 24 qubits. Overall, we were able to converge four systems to the FCI/CBS limit including He, Be, H₂, and LiH. We were also able to provide accurate dissociation curves for H₂, LiH, and N₂. Such computations required the use of only a single GPU. Since most quantum chemistry studies are presently out of reach of quantum computers, this research opens the path to more affordable quantitative quantum chemistry simulations of small molecules using QC algorithms. Thus, *a posteriori* corrections can be virtually added to any type of STO-3G VQE fermionic computations on real hardware [5, 48, 49] allowing us to improve significantly their accuracy at very little computational cost. Since adaptive simulations on real hardware are making some progress [50] while hardware itself improves, high-resolution corrected simulations should be progressively possible on future quantum computers providing a route to FCI quality computations. This strategy is particularly suited for resources demanding computations that converge slowly and require large basis sets associated to large qubits counts. Finally, DBBSC approaches are not limited to ground-state computations and can be extended to excited states via a linear response formalism[15]. This will be the subject of future research in the context of quantum computing. In that context, beside the state-of-the-art ADAPT-VQE hybrid quantum-classical algorithm, it would be interesting to revisit accurate fixed-ansätze [51], such as UCCSDT [52] (and others), to analyze their convergence when coupled to the DBBSC method. In practice, the presented DFT basis-set correction framework is not restricted to a given QC ansatz and can leverage any future QC algorithmic improvements. Thus, our present DBBSC/SABS methodology still requires to use qubits either through quantum hardware or through the use of a classical quantum emulator. The qubit count is therefore our main limitation. The computations of this paper used up to 32 qubits and represent a proof-of-concept study of what one can do with quantum emulation. However, state-vector simulations have limitations due to memory. Indeed, if they are theoretically possible up to 40-50 qubits on very large exascale supercomputers, they start to become relatively unpractical for chemical simulations when reaching 36 qubits due to the high computational resources and time-to-solution requirements. To explore further the chemical space with quantum algorithms, we are currently upgrading our Hyperion-1 framework to increase our emulated qubit counts by going beyond the state-vector formalism thanks to various elements from the CUDA-Q SDK [53, 54] developed by NVIDIA. We

are also presently testing various implementations of the DBBSC algorithms on available quantum hardware. To conclude, by reducing the number of qubits required to reach the CBS limit, we expect to tackle predictive real-world quantum chemistry applications with strategies applicable to both NISQ and FTQC quantum computing algorithms.

Acknowledgment

We thank the PEPR EPIQ - Quantum Software (ANR-22-PETQ-0007, J.-P.P.) for funding D. Traore's postdoctoral position. I.-M. Lygatsika's PhD position has been funded by the European Research Council (ERC) under the European Union's Horizon 2020 research and innovation program (grant No 810367, project EMC2, J.-P. P. and Y.M.). Computations have been performed at IDRIS (Jean Zay) on GENCI Grant no A0150712052 (J.-P.P.), at Scaleway (Jero) and on the SuperPOD reference cluster EOS at NVIDIA. The authors thank D. Ruau and C. Hundt (NVIDIA) for continuous support, as well as the NVIDIA Quantum team for technical discussions.

-
- [1] A. Y. Kitaev, "Quantum measurements and the abelian stabilizer problem," *arXiv preprint quant-ph/9511026*, 1995.
- [2] A. Aspuru-Guzik, A. D. Dutoi, P. J. Love, and M. Head-Gordon, "Simulated quantum computation of molecular energies," *Science*, vol. 309, no. 5741, pp. 1704–1707, 2005.
- [3] M. A. Nielsen and I. L. Chuang, *Quantum computation and quantum information*. Cambridge University Press, 2010.
- [4] J. D. Whitfield, J. Biamonte, and A. Aspuru-Guzik, "Simulation of electronic structure hamiltonians using quantum computers," *Molecular Physics*, vol. 109, no. 5, pp. 735–750, 2011.
- [5] A. Peruzzo, J. McClean, P. Shadbolt, M.-H. Yung, X.-Q. Zhou, P. J. Love, A. Aspuru-Guzik, and J. L. O'Brien, "A variational eigenvalue solver on a photonic quantum processor," *Nature Communications*, vol. 5, no. 1, pp. 1–7, 2014.
- [6] J. Tilly, H. Chen, S. Cao, D. Picozzi, K. Setia, Y. Li, E. Grant, L. Wossnig, I. Rungger, G. H. Booth, *et al.*, "The variational quantum eigensolver: a review of methods and best practices," *Physics Reports*, vol. 986, pp. 1–128, 2022.
- [7] P.-F. Loos, B. Pradines, A. Scemama, J. Toulouse, and E. Giner, "A density-based basis-set correction for wave function theory," *Journal of Physical Chemistry Letters*, vol. 10, no. 11, pp. 2931–2937, 2019.
- [8] E. Giner, B. Pradines, A. Ferté, R. Assaraf, A. Savin, and J. Toulouse, "Curing basis-set convergence of wavefunction theory using density-functional theory: A systematically improvable approach," *Journal of Chemical Physics*, vol. 149, p. 194301, 2018.
- [9] E. Giner, A. Scemama, J. Toulouse, and P.-F. Loos, "Chemically accurate excitation energies with small basis sets," *Journal of Chemical Physics*, vol. 151, no. 14, p. 144118, 2019.
- [10] P.-F. Loos, B. Pradines, A. Scemama, E. Giner, and J. Toulouse, "Density-Based Basis-Set Incompleteness Correction for GW Methods," *Journal of Chemical Theory and Computation*, vol. 16, pp. 1018–1028, Feb. 2020.
- [11] E. Giner, A. Scemama, P.-F. Loos, and J. Toulouse, "A basis-set error correction based on density-functional theory for strongly correlated molecular systems," *Journal of Chemical Physics*, vol. 152, p. 174104, May 2020.
- [12] E. Giner, D. Traore, B. Pradines, and J. Toulouse, "Self-consistent density-based basis-set correction: How much do we lower total energies and improve dipole moments?," *Journal of Chemical Physics*, vol. 155, p. 044109, Jul 2021.
- [13] D. Traore, E. Giner, and J. Toulouse, "Basis-set correction based on density-functional theory: Rigorous framework for a one-dimensional model," *The Journal of Chemical Physics*, vol. 156, no. 4, 2022.
- [14] D. Traore, J. Toulouse, and E. Giner, "Basis-set correction for coupled-cluster estimation of dipole moments," *The Journal of Chemical Physics*, vol. 156, no. 17, 2022.
- [15] D. Traore, E. Giner, and J. Toulouse, "Basis-set correction based on density-functional theory: Linear-response formalism for excited-state energies," *The Journal of Chemical Physics*, vol. 158, no. 23, 2023.
- [16] A. Hesselmann, E. Giner, P. Reinhardt, P. Knowles, H.-J. Werner, and J. Toulouse, "A density-fitting implementation of the density-based basis-set correction method," *Journal of Computational Chemistry*, 2024.
- [17] T. H. Dunning, "Gaussian basis sets for use in correlated molecular calculations. i. the atoms boron through neon and hydrogen," *Journal of Chemical Physics*, vol. 90, p. 1007, 1989.
- [18] F. Jensen, "Unifying general and segmented contracted basis sets. Segmented polarization consistent basis sets," *Journal of chemical theory and computation*, vol. 10, no. 3, pp. 1074–1085, 2014.
- [19] F. Aquilante, L. Boman, J. Boström, H. Koch, R. Lindh, A. S. de Merás, and T. B. Pedersen, "Cholesky decomposition techniques in electronic structure theory," *Linear-Scaling Techniques in Computational Chemistry and Physics: Methods and Applications*, pp. 301–343, 2011.
- [20] T. B. Pedersen, S. Lehtola, I. Fdez. Galván, and R. Lindh, "The versatility of the Cholesky decomposition in electronic structure theory," *Wiley Interdisciplinary Reviews: Computational Molecular Science*, vol. 14, no. 1, p. e1692, 2024.
- [21] S. Lehtola, "Curing basis set overcompleteness with pivoted Cholesky decompositions," *The Journal of Chemical Physics*, vol. 151, no. 24, 2019.

- [22] O. Schutt and J. VandeVondele, “Machine learning adaptive basis sets for efficient large scale density functional theory simulation,” *Journal of Chemical Theory and Computation*, vol. 14, no. 8, pp. 4168–4175, 2018.
- [23] Y. Mao, P. R. Horn, N. Mardirossian, T. Head-Gordon, C.-K. Skylaris, and M. Head-Gordon, “Approaching the basis set limit for DFT calculations using an environment-adapted minimal basis with perturbation theory: Formulation, proof of concept, and a pilot implementation,” *The Journal of Chemical Physics*, vol. 145, no. 4, 2016.
- [24] W. Wang and J. D. Whitfield, “Basis set generation and optimization in the nisq era with quiqbox.jl,” *Journal of Chemical Theory and Computation*, vol. 19, no. 22, pp. 8032–8052, 2023. PMID: 37924295.
- [25] H.-Y. Kwon, G. M. Curtin, Z. Morrow, C. Kelley, and E. Jakubikova, “Adaptive basis sets for practical quantum computing,” *International Journal of Quantum Chemistry*, vol. 123, no. 14, p. e27123, 2023.
- [26] J. S. Kottmann, P. Schleich, T. Tamayo-Mendoza, and A. Aspuru-Guzik, “Reducing qubit requirements while maintaining numerical precision for the variational quantum eigensolver: A basis-set-free approach,” *The Journal of Physical Chemistry Letters*, vol. 12, no. 1, pp. 663–673, 2021. PMID: 33393305.
- [27] E. Posenitskiy, V. G. Chilkuri, A. Ammar, M. Hapka, K. Pernal, R. Shinde, E. J. Landinez Borda, C. Filippi, K. Nakano, O. Kohulák, *et al.*, “TREXIO: A file format and library for quantum chemistry,” *The Journal of Chemical Physics*, vol. 158, no. 17, 2023.
- [28] I.-M. Lygatsika, *Méthodes numériques pour les discrétisations Gaussiennes des problèmes en structure électronique*. Phd thesis, Sorbonne Université, Paris, France, October 2023.
- [29] S. R. Jensen, S. Saha, J. A. Flores-Livas, W. Huhn, V. Blum, S. Goedecker, and L. Frediani, “The Elephant in the Room of Density Functional Theory Calculations,” *The Journal of Physical Chemistry Letters*, vol. 8, no. 7, pp. 1449–1457, 2017. PMID: 28291362.
- [30] C. Lucas, “LAPACK-style codes for level 2 and 3 pivoted Cholesky factorizations,” *LAPACK Working*, vol. 4, no. 5, 2004.
- [31] Y. S. Yordanov, V. Armaos, C. H. Barnes, and D. R. Arvidsson-Shukur, “Qubit-excitation-based adaptive variational quantum eigensolver,” *Communications Physics*, vol. 4, no. 1, pp. 1–11, 2021.
- [32] O. Adjoua and C. Feniou, “Sorbonne Université, cnrs and Qubit Pharmaceuticals,” 2023.
- [33] B. Huron, J. Malrieu, and P. Rancurel, “Iterative perturbation calculations of ground and excited state energies from multiconfigurational zeroth-order wavefunctions,” *The Journal of Chemical Physics*, vol. 58, no. 12, pp. 5745–5759, 1973.
- [34] C. Feniou, M. Hassan, D. Traoré, E. Giner, Y. Maday, and J.-P. Piquemal, “Overlap-ADAPT-VQE: Practical Quantum Chemistry on Quantum Computers via Overlap-Guided Compact Ansätze,” *Communications Physics*, vol. 6, 2023.
- [35] C. Feniou, O. Adjoua, B. Claudon, J. Zylberman, E. Giner, and J.-P. Piquemal, “Sparse quantum state preparation for strongly correlated systems,” *The Journal of Physical Chemistry Letters*, vol. 15, no. 11, pp. 3197–3205, 2024.
- [36] T. Helgaker, W. Klopper, H. Koch, and J. Noga, “Basis-set convergence of correlated calculations on water,” *The Journal of Chemical Physics*, vol. 106, no. 23, pp. 9639–9646, 1997.
- [37] I. Kassal and A. Aspuru-Guzik, “Quantum algorithm for molecular properties and geometry optimization,” *The Journal of Chemical Physics*, vol. 131, no. 22, 2009.
- [38] Y. Garniron, T. Applencourt, K. Gasperich, A. Benali, A. Ferté, J. Paquier, B. Pradines, R. Assaraf, P. Reinhardt, J. Toulouse, P. Barbaresco, N. Renon, G. David, J.-P. Malrieu, M. Véril, M. Caffarel, P.-F. Loos, E. Giner, and A. Scemama, “Quantum Package 2.0: An Open-Source Determinant-Driven Suite of Programs,” *Journal of Chemical Theory and Computation*, vol. 15, no. 6, pp. 3591–3609, 2019. PMID: 31082265.
- [39] B. Huron, J. P. Malrieu, and P. Rancurel, “Iterative perturbation calculations of ground and excited state energies from multiconfigurational zeroth-order wavefunctions,” *Journal of Chemical Physics*, vol. 58, pp. 5745–5759, Jun 1973.
- [40] J. A. Pople, *Modern theoretical chemistry*. Plenum, New York, 1976.
- [41] E. R. Davidson and D. Feller, “Basis set selection for molecular calculations,” *Chemical Reviews*, vol. 86, no. 4, pp. 681–696, 1986.
- [42] N. M. Tubman, C. Mejuto-Zaera, J. M. Epstein, D. Hait, D. S. Levine, W. Huggins, Z. Jiang, J. R. McClean, R. Babbush, M. Head-Gordon, and K. B. Whaley, “Postponing the orthogonality catastrophe: efficient state preparation for electronic structure simulations on quantum devices,” *arXiv preprint arXiv:1809.05523*, 2018.
- [43] J. Almlöf, B. J. Deleeuw, P. R. Taylor, C. W. Bauschlicher Jr, and P. Siegbahn, “The dissociation energy of N₂,” *International Journal of Quantum Chemistry*, vol. 36, no. S23, pp. 345–354, 1989.
- [44] K. A. Peterson and T. H. Dunning Jr, “Intrinsic errors in several ab initio methods: the dissociation energy of N₂,” *The Journal of Physical Chemistry*, vol. 99, no. 12, pp. 3898–3901, 1995.
- [45] J. Robledo-Moreno, M. Motta, H. Haas, A. Javadi-Abhari, P. Jurcevic, W. Kirby, S. Martiel, K. Sharma, S. Sharma, T. Shirakawa, *et al.*, “Chemistry beyond exact solutions on a quantum-centric supercomputer,” *arXiv preprint arXiv:2405.05068*, 2024.
- [46] J. Provazza, K. Gunst, H. Zhai, G. K.-L. Chan, T. Shiozaki, N. C. Rubin, and A. F. White, “Fast emulation of fermionic circuits with matrix product states,” *Journal of Chemical Theory and Computation*, 2024. DOI: 10.1021/acs.jctc.4c00200.
- [47] A. Halkier, W. Klopper, T. Helgaker, and P. Jørgensen, “Basis-set convergence of the molecular electric dipole moment,” *The Journal of Chemical Physics*, vol. 111, no. 10, pp. 4424–4430, 1999.
- [48] A. Kandala, A. Mezzacapo, K. Temme, M. Takita, M. Brink, J. M. Chow, and J. M. Gambetta, “Hardware-efficient variational quantum eigensolver for small molecules and quantum magnets,” *Nature*, vol. 549, no. 7671, pp. 242–246, 2017.
- [49] W. Sennane, J.-P. Piquemal, and M. J. Rančić, “Calculating the ground-state energy of benzene under spatial deformations with noisy quantum computing,” *Physical Review A*, vol. 107, no. 1, p. 012416, 2023.
- [50] C. Feniou, B. Claudon, M. Hassan, A. Courtat, O. Adjoua, Y. Maday, and J.-P. Piquemal, “Greedy gradient-

- free adaptive variational quantum algorithms on a noisy intermediate scale quantum computer,” *arXiv preprint arXiv:2306.17159*, 2023.
- [51] M. Haidar, M. J. Rančić, T. Ayrat, Y. Maday, and J.-P. Piquemal, “Open source variational quantum eigensolver extension of the quantum learning machine for quantum chemistry,” *WIREs Computational Molecular Science*, vol. 13, no. 5, p. e1664, 2023.
- [52] M. Haidar, M. J. Rančić, Y. Maday, and J.-P. Piquemal, “Extension of the trotterized unitary coupled cluster to triple excitations,” *The Journal of Physical Chemistry A*, vol. 127, no. 15, pp. 3543–3550, 2023.
- [53] H. Bayraktar, A. Charara, D. Clark, S. Cohen, T. Costa, Y.-L. L. Fang, Y. Gao, J. Guan, J. Gunnels, A. Haidar, *et al.*, “cuquantum sdk: A high-performance library for accelerating quantum science,” in *2023 IEEE International Conference on Quantum Computing and Engineering (QCE)*, vol. 1, pp. 1050–1061, IEEE, 2023.
- [54] J.-S. Kim, A. McCaskey, B. Heim, M. Modani, S. Stanwyck, and T. Costa, “Cuda quantum: The platform for integrated quantum-classical computing,” in *2023 60th ACM/IEEE Design Automation Conference (DAC)*, pp. 1–4, IEEE, 2023.